Particle–hole bound states of dipolar molecules in an optical lattice*

Zhang Yi-Cai(张义财)[a)†], Wang Han-Ting(汪汉廷)[a)], Shen Shun-Qing(沈顺清)[b)], and Liu Wu-Ming(刘伍明)[a)]

[a)] *Beijing National Laboratory for Condensed Matter Physics, Institute of Physics, Chinese Academy of Sciences, Beijing* 100190, *China*
[b)] *Department of Physics and Centre of Theoretical and Computational Physics, The University of Hong Kong, Hong Kong, China*

(Received 15 March 2013; revised manuscript received 15 April 2013)

We investigate the particle–hole pair excitations of dipolar molecules in an optical lattice, which can be described with an extended Bose–Hubbard model. For strong enough dipole–dipole interaction, the particle–hole pair excitations can form bound states in one and two dimensions. With decreasing dipole-dipole interaction, the energies of the bound states increase and merge into the particle–hole continuous spectrum gradually. The existence regions, the energy spectra and the wave functions of the bound states are carefully studied and the symmetries of the bound states are analyzed with group theory. For a given dipole–dipole interaction, the number of bound states varies in momentum space and a number distribution of the bound states is illustrated. We also discuss how to observe these bound states in future experiments.

Keywords: particle–hole exications, bound states, dipolar molecules

PACS: 05.30.Jp, 03.75.Hh, 03.65.Ge **DOI:** 10.1088/1674-1056/22/9/090501

1. Introduction

Cold and ultracold molecules are attracting more and more attention due to their broad applications in the fields of high-precision measurement, quantum chemistry, quantum information, and many-body physics.[1,2] In recent years, experimental techniques using cold and ultracold molecules have been developed greatly. The homonuclear molecular Bose–Einstein condensation (BEC) was realized experimentally[3,4] and the quantum state with exactly one molecule at each site of an optical lattice was created with a Feshbach resonance and STIRAP (stimulated Raman adiabatic passage) techniques.[5,6] Meanwhile, ultracold heteronuclear molecules were also produced.[7–11]

Heteronuclear molecules, such as SrO, RbCs, or NaCs, prepared in their electronic and vibrational ground states, have a considerable permanent electric dipole moment. The dipole–dipole interaction between molecules can be generated by the external applied electric field.[1,2] Moreover, the magnitude of the dipole–dipole interaction can be controlled by the strength of the electric field.[12,13] The tunable long range dipole–dipole interaction may significantly modify the ground state and collective excitations of trapped condensates. For example, in trapped dipolar gases, it was shown theoretically[14] that the mean-field inter-particle interaction and the stability diagram are governed by the trapping geometry. With the increase of the dipolar interaction, the ground state of rotating atomic Bose gases undergoes a series of transitions between vortex lattices of different symmetries: triangular, square, "stripe", and "bubble" phases.[15] In rapidly rotating Fermion gas, the dipole–dipole interaction may even result in fractional quantum Hall-like states.[16]

The particles with long-range interactions in an optical lattice can be described with the extended Hubbard model.[17–19] Compared with the regular Bose–Hubbard model with on-site interaction, the extended Bose–Hubbard model has richer ground state phases, such as Mott insulator, particle density wave, superfluidity or supersolid phases.[20–28] On the other hand, the gapful particle and hole excitations in the insulating phase[29–31] may bind together and form bound states due to long-range interactions. Although the excitons (holon–doublon pairs) in the one-dimensional fermionic Hubbard model have been studied,[32–34] the excitons in bosonic molecules are less studied.

In this paper, we study the particle–hole pair excitations of dipolar bosonic molecules in an optical lattice, especially, the possible bound states due to the dipole–dipole interaction. The paper is organized as follows. In Section 2, we introduce the extended Bose–Hubbard model to describe the polarized bosonic molecules in an optical lattice, and derive the eigen equations to describe the single particle–hole pair excitation. In Section 3, the existence regions, the energies and the wave functions of the particle–hole bound states are calculated in one and two dimensions. The symmetries of the bound states are analyzed and possible experimental observation of these bound states is also discussed. A summary is presented in Section 4.

*Project supported by the National Basic Research Program of China (Grant Nos. 2011CB921502), the National Natural Science Foundation of China (Grant No. 10934010), and the Joint Research Projects of the National Natural Science Foundation of China and Hong Kong Research Grant Council (Grant Nos. 11061160490 and N-HKU748/10).

†Corresponding author. E-mail: zhangyicai123456@163.com

© 2013 Chinese Physical Society and IOP Publishing Ltd

2. Particle–hole bound states in extended Bose–Hubbard model

Considering only the nearest-neighbor interaction V to simulate the effect of dipole–dipole interaction, we write the extended Bose–Hubbard model as

$$\begin{aligned} H &= H_0 + H_1, \\ H_0 &= \frac{U}{2}\sum_{\boldsymbol{r}} n_{\boldsymbol{r}}(n_{\boldsymbol{r}}-1) + \frac{V}{2}\sum_{\boldsymbol{r},\boldsymbol{\delta}} n_{\boldsymbol{r}} n_{\boldsymbol{r}+\boldsymbol{\delta}}, \\ H_1 &= -t\sum_{\boldsymbol{r},\boldsymbol{\delta}} (b^{\dagger}_{\boldsymbol{r}} b_{\boldsymbol{r}+\boldsymbol{\delta}}), \end{aligned} \tag{1}$$

where $n_{\boldsymbol{r}} = b^{\dagger}_{\boldsymbol{r}} b_{\boldsymbol{r}}$ is the number operator at site $\boldsymbol{r}$ with $b_{\boldsymbol{r}}(b^{\dagger}_{\boldsymbol{r}})$ the annihilation (creation) operator of particle, $\boldsymbol{\delta}$ denotes the nearest neighbor vectors of site $\boldsymbol{r}$. The on-site interaction U, the nearest neighbor interaction V and the hopping t are expressed as

$$\begin{aligned} U &= g\int \mathrm{d}\boldsymbol{x}|W(\boldsymbol{x})|^4, \\ V &= \int \mathrm{d}\boldsymbol{x}\mathrm{d}\boldsymbol{x}'|W(\boldsymbol{x}-\boldsymbol{r})|^2 V_{\mathrm{dd}}(\boldsymbol{x}-\boldsymbol{x}')|W(\boldsymbol{x}'-(\boldsymbol{r}+\boldsymbol{\delta}))|^2, \\ t &= -\int \mathrm{d}\boldsymbol{x} W^*(\boldsymbol{x}-\boldsymbol{r})\left[-\frac{\hbar^2}{2m}\nabla^2 + V_0(\boldsymbol{x})\right] \\ &\quad \times W(\boldsymbol{x}-(\boldsymbol{r}+\boldsymbol{\delta})), \end{aligned} \tag{2}$$

where $W(\boldsymbol{r})$ is Wannier function corresponding to the lowest energy band and

$$V_{\mathrm{dd}}(\boldsymbol{x}) = \frac{C_{\mathrm{dd}}}{4\pi}\frac{1-3\cos^2\theta}{|\boldsymbol{x}|^3}$$

is the dipole–dipole interaction of two particles separated with a distance $|\boldsymbol{x}|$. For the electric dipole–dipole interaction, $C_{\mathrm{dd}} = d^2/\varepsilon_0$ with d the electric dipole moment, ε_0 is vacuum permittivity. We assume that the polarization of dipole moment is along the z-axial direction. In the following studies, we consider particles confined in a one-dimensional chain or a two-dimensional square lattice and treat the hopping term H_1 as a perturbation.

In the atomic limit ($t = 0$), $n_{\boldsymbol{r}}$ is a good quantum number and the eigenstates of H_0 can be written as the direct product of number states. When the filling factor is one, $V \geq 0$ and $zV < U$, the Mott insulating ground state can be written as $|11111111\ldots\rangle$ with the ground state energy $E_0 = NzV/2$, where z is the coordination number and N is the number of lattice sites. The excited states contain one or more particle–hole pairs. A single particle–hole pair state with a hole at r and a particle at r' can be represented as $|r,r'\rangle = |110_r111112_{r'}11\ldots\rangle$. Taking into account the hopping term t, the particle and hole will move in the lattice. Similar to the two-magnon states in a ferromagnetic system,[35] the single particle–hole pair state can be written as a linear combination of $|r,r'\rangle$:

$$|\psi\rangle = \sum_{\boldsymbol{r},\boldsymbol{r}'} \phi_{\boldsymbol{r},\boldsymbol{r}'}|\boldsymbol{r},\boldsymbol{r}'\rangle, \tag{3}$$

where $\phi_{\boldsymbol{r},\boldsymbol{r}'}$ will be determined by solving the approximate eigen equation in single particle–hole pair subspace

$$\langle \boldsymbol{r},\boldsymbol{r}'|H|\psi\rangle = E\langle \boldsymbol{r},\boldsymbol{r}'|\psi\rangle. \tag{4}$$

Calculating $H|\boldsymbol{r},\boldsymbol{r}'\rangle$ and considering the boundary condition $\phi_{\boldsymbol{r},\boldsymbol{r}} = 0$ (a particle and a hole do not share the same lattice site), we obtain

$$\begin{aligned} &-\sum_{\boldsymbol{\delta}}(t\phi_{\boldsymbol{r}+\boldsymbol{\delta},\boldsymbol{r}'} + 2t\phi_{\boldsymbol{r},\boldsymbol{r}'+\boldsymbol{\delta}}) = \varepsilon\phi_{\boldsymbol{r},\boldsymbol{r}'} \\ &+\sum_{\boldsymbol{\delta}}\delta_{\boldsymbol{r}'-\boldsymbol{r},\boldsymbol{\delta}}[V\phi_{\boldsymbol{r},\boldsymbol{r}'} + (-t)\phi_{\boldsymbol{r}+\boldsymbol{\delta},\boldsymbol{r}'} + (-2t)\phi_{\boldsymbol{r},\boldsymbol{r}'-\boldsymbol{\delta}}] \\ &-\delta_{\boldsymbol{r}'-\boldsymbol{r},0}\sum_{\boldsymbol{\delta}}(t\phi_{\boldsymbol{r}+\boldsymbol{\delta},\boldsymbol{r}'} + 2t\phi_{\boldsymbol{r},\boldsymbol{r}'+\boldsymbol{\delta}}), \end{aligned} \tag{5}$$

where $\delta_{\boldsymbol{r}'-\boldsymbol{r},\delta}$ is the Kronecker delta function and $\varepsilon = E - E_0 - U$. The particle–hole excitation energy is $\omega = E - E_0 = \varepsilon + U$.

Owing to the translational invariance, it is convenient to apply a transformation $\phi_{\boldsymbol{r},\boldsymbol{r}'} = \mathrm{e}^{\mathrm{i}\boldsymbol{K}\cdot\boldsymbol{R}}\phi(\boldsymbol{\rho})/\sqrt{N}$, where $\boldsymbol{R} = (\boldsymbol{r}+\boldsymbol{r}')/2$ and $\boldsymbol{\rho} = \boldsymbol{r}' - \boldsymbol{r}$ denote the center-of-mass and the relative coordinates respectively and $\boldsymbol{K}$ the total momentum of the particle and hole. At fixed $\boldsymbol{K}$, the eigen equation (5) becomes

$$\begin{aligned} &-\sum_{\boldsymbol{\delta}}[t\mathrm{e}^{\mathrm{i}\boldsymbol{K}\cdot\boldsymbol{\delta}/2}\phi(\boldsymbol{\rho}-\boldsymbol{\delta}) + 2t\mathrm{e}^{\mathrm{i}\boldsymbol{K}\cdot\boldsymbol{\delta}/2}\phi(\boldsymbol{\rho}+\boldsymbol{\delta})] \\ &= \varepsilon\phi(\boldsymbol{\rho}) + \sum_{\boldsymbol{\delta}}\delta_{\boldsymbol{\rho},\boldsymbol{\delta}}[V\phi(\boldsymbol{\rho}) \\ &\quad +(-t\mathrm{e}^{\mathrm{i}\boldsymbol{K}\cdot\boldsymbol{\delta}/2} - 2t\mathrm{e}^{-\mathrm{i}\boldsymbol{K}\cdot\boldsymbol{\delta}/2})\phi(\boldsymbol{\rho}-\boldsymbol{\delta})] \\ &\quad -\delta_{\boldsymbol{\rho},0}\sum_{\boldsymbol{\delta}}[t\mathrm{e}^{-\mathrm{i}\boldsymbol{K}\cdot\boldsymbol{\delta}/2}\phi(\boldsymbol{\delta}) + 2t\mathrm{e}^{\mathrm{i}\boldsymbol{K}\cdot\boldsymbol{\delta}/2}\phi(\boldsymbol{\delta})]. \end{aligned} \tag{6}$$

Considering the finite range character of the nearest neighbor interaction V, we utilize the Green function approach to solve the eigen equation. To this end, we introduce an effective Hamiltonian

$$H_{\mathrm{eff}} = H_{\mathrm{ph},0} + V_{\mathrm{ph}}, \tag{7}$$

where

$$\begin{aligned} H_{\mathrm{ph},0} &= -t\sum_{\boldsymbol{\rho},\boldsymbol{\delta}}\mathrm{e}^{\mathrm{i}\boldsymbol{K}\cdot\boldsymbol{\delta}/2}|\boldsymbol{\rho}\rangle\langle\boldsymbol{\rho}-\boldsymbol{\sigma}| - 2t\mathrm{e}^{\mathrm{i}\boldsymbol{K}\cdot\boldsymbol{\delta}/2}|\boldsymbol{\rho}\rangle\langle\boldsymbol{\rho}+\boldsymbol{\delta}|, \\ V_{\mathrm{ph}} &= \sum_{\boldsymbol{\delta}}(2t\mathrm{e}^{-\mathrm{i}\boldsymbol{K}\cdot\boldsymbol{\delta}/2} + t\mathrm{e}^{\mathrm{i}\boldsymbol{K}\cdot\boldsymbol{\delta}/2})|\boldsymbol{\delta}\rangle\langle 0| + h.c. \\ &\quad +\sum_{\boldsymbol{\delta}}(-V)|\boldsymbol{\delta}\rangle\langle\boldsymbol{\delta}| \end{aligned}$$

to describe the motion of a particle around a hole, where $|\boldsymbol{\rho}\rangle$ is the basis set in relative coordinate spaces. The $\boldsymbol{K}$-dependent $H_{\mathrm{ph},0}$ describes the kinetic energy of the particle and V_{ph} denotes the interaction between the particle and hole. With $|\phi\rangle = \sum_{\boldsymbol{\rho}}\phi(\boldsymbol{\rho})|\boldsymbol{\rho}\rangle$, it is easy to reproduce Eq. (6) from the

eigen equation $H_{\rm eff}|\phi\rangle = \varepsilon|\phi\rangle$. After a Fourier transformation, the kinetic energy is obtained as

$$\varepsilon_0(\boldsymbol{K},\boldsymbol{q}) = -t\sum_{\boldsymbol{\delta}} e^{i(\boldsymbol{K}/2+\boldsymbol{q})\cdot\boldsymbol{\delta}} - 2t\sum_{\boldsymbol{\delta}} e^{i(\boldsymbol{K}/2-\boldsymbol{q})\cdot\boldsymbol{\delta}}, \quad (8)$$

where $\boldsymbol{q}$ is the relative momentum of a particle and a hole. When a particle is adjacent to a hole, the energy offset $-V$ in $V_{\rm ph}$ may result in the formation of particle–hole bound states.

Introducing retarded Green functions $G_0 = \lim_{\eta\to 0^+} 1/(\varepsilon - H_{\rm ph,0} + i\eta)$ and $G = \lim_{\eta\to 0^+} 1/(\varepsilon - H_{\rm eff} + i\eta)$, we could calculate G through the Lippmann–Schwinger equation $G = G_0 + G_0 V_{\rm ph} G$. In the real space, the Green function G has a general form

$$\langle\boldsymbol{\rho}'|G|\boldsymbol{\rho}\rangle = \lim_{\eta\to 0^+}\sum_m \frac{\phi_m(\boldsymbol{\rho}')\phi_m^*(\boldsymbol{\rho})}{\varepsilon - E_m + i\eta} = G(\boldsymbol{\rho}',\boldsymbol{\rho},\varepsilon),$$

where the contributions of the continuous spectra are neglected and E_ms are the eigenvalues of the bound states with ϕ_ms the corresponding eigenfunctions.[36] We can determine the eigenvalues and eigenfunctions by analyzing the poles and residues of the obtained Green's function.

From Eq. (7), we have

$$\langle\boldsymbol{\rho}'|G_0|\boldsymbol{\rho}\rangle = \lim_{\eta\to 0^+}\frac{1}{(2\pi)^d}\int_{-\pi}^{\pi}\frac{d^d q e^{i\boldsymbol{q}\cdot(\boldsymbol{\rho}'-\boldsymbol{\rho})}}{\varepsilon - \varepsilon_0(\boldsymbol{K},\boldsymbol{q}) + i\eta},$$

and

$$\langle\boldsymbol{\rho}'|G|\boldsymbol{\rho}\rangle = \langle\boldsymbol{\rho}'|G_0|\boldsymbol{\rho}\rangle + \sum_{\boldsymbol{\rho}_1,\boldsymbol{\rho}_2}\langle\boldsymbol{\rho}'|G_0|\boldsymbol{\rho}_1\rangle\langle\boldsymbol{\rho}_1|V_{\rm ph}|\boldsymbol{\rho}_2\rangle\langle\boldsymbol{\rho}_2|G|\boldsymbol{\rho}\rangle. \quad (9)$$

For specific $\boldsymbol{\rho\prime} = 0$ or $\boldsymbol{\delta}$, equation (9) can be reduced to a set of simultaneous linear equations. Green functions $\langle\boldsymbol{\rho}'|G|\boldsymbol{\rho}\rangle$ with $\boldsymbol{\rho\prime} = 0$ or $\boldsymbol{\delta}$ can thus be obtained exactly. The residues of $\langle 0|G|\boldsymbol{\rho}\rangle$ always vanish for non-vanishing bound states energies ε in our calculations, which is consistent with the boundary condition $\phi(0) = 0$. We present our results in the next section.

3. Bound states in one and two dimensions

3.1. Bound states in one dimension

In the Mott insulating phase, the excitation energy of a single particle/hole was calculated as

$$\omega_{\rm p,h} = \pm\left[-\frac{\varepsilon_0}{2} + U\left(n_0 - \frac{1}{2}\right) + 2dVn_0 - \mu\right] + \left[\left(\frac{\varepsilon_0}{2}\right)^2 + \varepsilon_0 U\left(n_0 + \frac{1}{2}\right) + \frac{U^2}{4}\right]^{1/2}, \quad (10)$$

with the dynamical Gutzwiller approach.[31] Up to the first order of t/U, the single particle–hole pair excitation energy is

$$\omega = \omega_p(\boldsymbol{k}_p) + \omega_{\rm h}(\boldsymbol{k}_{\rm h}) = U + \varepsilon_0(\boldsymbol{K},\boldsymbol{q}), \quad (11)$$

with the total momentum $\boldsymbol{K} = \boldsymbol{k}_{\rm p} + \boldsymbol{k}_{\rm h}$ and relative momentum $\boldsymbol{q} = (\boldsymbol{k}_{\rm h} - \boldsymbol{k}_{\rm p})/2$. For the extended Bose–Hubbard model, however, a particle–hole pair may form a bound state due to the interaction [See Eq. (7)]. In the following calculations, we take the lattice constant as 1 and use $t > 0$ as the unit of energy. Conditions of $t/U \ll 1$ and $zV < U$ are assumed to make sure that the ground state of the system is the deep Mott insulating phase.

In the one-dimensional case, $\varepsilon_0(\boldsymbol{K},\boldsymbol{q}) = -2t_{\hat{x}}\cos(q + \theta_{\hat{x}})$ with $t_{\hat{x}} = t\sqrt{9\cos^2(K_x/2) + \sin^2(K_x/2)}$ and $\theta_{\hat{x}} = \arctan[\tan(K_x/2)/3]$. The top and bottom boundaries of particle–hole continuous spectrum are

$$\Omega_1^{t(b)}(K) = \pm 2t_{\hat{x}}, \quad (12)$$

(see Fig. 1). Compared with particle–hole pairs in fermion Hubbard model with half filling,[38] the minimum of bandwidth of the continuous spectrum is non-zero at $K = \pm\pi$. This is because that there is no particle–hole symmetry in the Bose–Hubbard model.

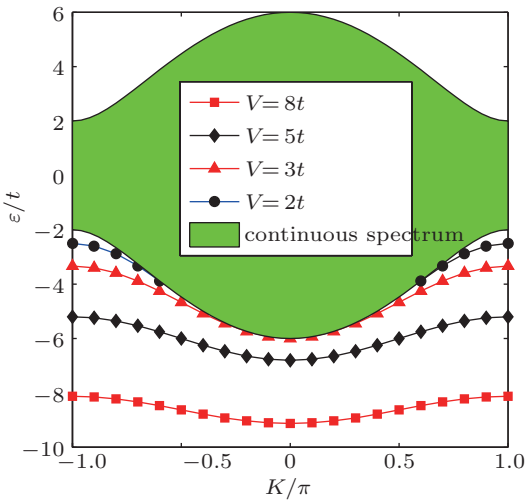


Fig. 1. (color online) Energy spectra of the bound states of a particle–hole pair in one dimension for different nearest-neighbor interactions $V = 2t$ (black circles), $V = 3t$ (red triangles), $V = 5t$ (black diamonds) and $V = 8t$ (red squares) respectively ($K = K_x$). As a comparison, the continuous spectrum of a particle–hole pair excitation is also shown (green shaded region).

For a specific nearest-neighbor interaction V and total momentum K, we search for bound state solutions outside the continuum. In the case of $\varepsilon < -2t_{\hat{x}}$, the free Green function is calculated as[37]

$$\langle\boldsymbol{\rho}'|G_0|\boldsymbol{\rho}\rangle = \lim_{\eta\to 0^+}\frac{1}{(2\pi)^d}\int_{-\pi}^{\pi}\frac{d^d q e^{i\boldsymbol{q}\cdot(\boldsymbol{\rho}'-\boldsymbol{\rho})}}{\varepsilon - \varepsilon_0(\boldsymbol{K},\boldsymbol{q}) + i\eta} = \alpha\beta^{|\boldsymbol{\rho}-\boldsymbol{\rho}'|}\gamma^{\boldsymbol{\rho}-\boldsymbol{\rho}'}, \quad (13)$$

where $\alpha = -1/\sqrt{\varepsilon^2 - 4t_{\hat{x}}^2}$, $\gamma = e^{i\theta_{\hat{x}}}$ and $\beta = e^{-\kappa}$ with $\kappa = \operatorname{arccosh}(|\varepsilon|/2t_{\hat{x}})$.

With $\rho' = 0, \pm 1$, equation (9) is reduced to three linear equations. The Green functions of $\langle -1|G|\boldsymbol{\rho}\rangle$, $\langle 0|G|\boldsymbol{\rho}\rangle$, and

$\langle 1|G|\rho\rangle$ can be exactly obtained as

$$\begin{aligned}
\langle -1|G|\rho\rangle &= \frac{\theta(-\rho)(\beta/\gamma)^{-(\rho+1)}}{-(t_{\hat{x}}-V\beta)/\beta}, \quad \rho \neq 0, \\
\langle 0|G|\rho\rangle &= 0, \\
\langle 1|G|\rho\rangle &= \frac{\theta(\rho)(\beta\gamma)^{\rho-1}}{-(t_{\hat{x}}-V\beta)/\beta}, \quad \rho \neq 0,
\end{aligned} \tag{14}$$

where $\theta(\rho)$ is the Heaviside step function. From these Green functions, we obtain two degenerate bound states corresponding to the particles on the left and right of the hole respectively. The bound state energy is

$$\varepsilon = -V - \frac{t_{\hat{x}}^2}{V}. \tag{15}$$

Accordingly, β is simplified as $\beta = t_{\hat{x}}/V < 1$ and the condition for the existence of the bound state is obtained as

$$V > t\sqrt{9\cos^2(\frac{K_x}{2}) + \sin^2(\frac{K_x}{2})}. \tag{16}$$

When $0 \leq V \leq t$, the interaction between a particle and a hole is too weak to bind them together and no bound state is found. When $t < V < 3t$, two degenerate bound states exist in the region of $2\arccos\sqrt{(V^2-t^2)/(8t^2)} < |K_x| \leq \pi$. The region becomes larger with the increase of V. When $V \geq 3t$, bound states may be found in the whole first Brillouin zone. In Fig.1, we show the spectra of the bound states for the interaction $V = 2t$, $3t$, $5t$, and $8t$, respectively. The energies of the bound states decrease with Vincreasing. At $V = 2t$, the calculated existence intervals are $0.58\pi < |K_x| \leq \pi$.

From the residues of the Green function, we can also extract the bound state wave functions. For example, the bound state with a particle on the right of a hole is written as

$$\begin{aligned}
\phi_R(\rho) &= C\left(\frac{t_{\hat{x}}}{V}\right)^{(\rho-1)} \mathrm{e}^{-\mathrm{i}\theta_{\hat{x}}(\rho-1)}, \quad \rho \geq 1, \\
\phi_R(\rho) &= 0, \quad \rho < 1,
\end{aligned} \tag{17}$$

where $C = \sqrt{1-(t_{\hat{x}}^2/V^2)}$ is the normalized constant. In Fig. 2, we show the probability distribution of the wave function for $K = 0$ and $V = 8t$.

The mean size of the bound state is calculated as $d = \langle\phi_R(\rho)|\rho|\phi_R(\rho)\rangle = V^2/(V^2-t_{\hat{x}}^2)$. In Fig. 3, we show the mean size of the bound state as a function of the nearest-neighbor interaction V at $K_x = 0$. The stronger the interaction, the smaller the size and the closer the particle and hole bind.

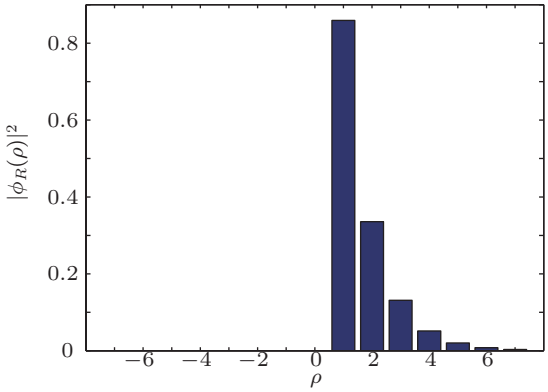


Fig. 2. (color online) Probability density of a bound state in real space in the case of $V = 8t$ and $K = 0$. The probability density decreases exponentially with the increase of distance.

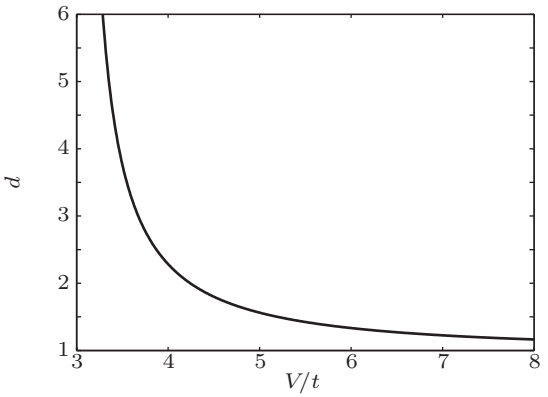


Fig. 3. The mean size d of bound states as a function of V at $K = 0$ in one dimension. When the nearest-neighbor interaction V approaches the critical value $V = 3t$, the mean size of the bound state becomes divergent and the bound state energies merge into a continuous spectrum (see the red triangles in Fig. 1), indicating the disintegration of the bound states.

3.2. Bound states in two dimensions

Before presenting the numerical results, we discuss the symmetries of the effective Hamiltonian H_{eff} in Eq. (7) in detail. After a gauge transformation

$$|\boldsymbol{\rho}\rangle' = |x,y\rangle' = \mathrm{e}^{-\mathrm{i}(x\theta_{\hat{x}}+y\theta_{\hat{y}})}|x,y\rangle = \mathrm{e}^{-\mathrm{i}(x\theta_{\hat{x}}+y\theta_{\hat{y}})}|\boldsymbol{\rho}\rangle, \tag{18}$$

with $\theta_{\hat{x}} = \arctan[\tan(K_x/2)/3]$ and $\theta_{\hat{y}} = \arctan[\tan(K_y/2)/3]$, we could remove the phase factors in the Hamiltonian and obtain

$$\begin{aligned}
H'_{\mathrm{eff}} &= H'_{\mathrm{ph},0} + V'_{\mathrm{ph}}, \\
H'_{\mathrm{ph},0} &= -t_{\hat{x}}\sum_{\boldsymbol{\rho},\boldsymbol{\delta}_x}|\boldsymbol{\rho}\rangle'\langle\boldsymbol{\rho}-\boldsymbol{\delta}_x|' - t_{\hat{y}}\sum_{\boldsymbol{\rho},\boldsymbol{\delta}_y}|\boldsymbol{\rho}\rangle'\langle\boldsymbol{\rho}-\boldsymbol{\delta}_y|', \\
V'_{\mathrm{ph}} &= -V\sum_{\boldsymbol{\delta}}|\boldsymbol{\delta}\rangle'\langle\boldsymbol{\delta}|' + t_{\hat{x}}\sum_{\boldsymbol{\delta}_x}|\boldsymbol{\delta}_x\rangle'\langle 0|' + \mathrm{h.c.} \\
&\quad + t_{\hat{y}}\sum_{\boldsymbol{\delta}_y}|\boldsymbol{\delta}_y\rangle'\langle 0|' + \mathrm{h.c.},
\end{aligned} \tag{19}$$

where $\boldsymbol{\delta}_x$ and $\boldsymbol{\delta}_y$ denote the nearest neighbors along the x and y directions, respectively, and

$$t_{\hat{x}} = t\sqrt{9\cos^2(K_x/2) + \sin^2(K_x/2)}$$

and

$$t_{\hat{y}} = t\sqrt{9\cos^2(K_y/2) + \sin^2(K_y/2)}$$

are effective hoppings along the x and y directions.

When $K_x = \pm K_y$, $t_{\hat{x}} = t_{\hat{y}}$, H'_{eff} has symmetries of the D_4 group. According to the irreducible representations of this group, the bound states can be classified and labeled with s, $p_{x(y)}$, and $d_{x^2-y^2}$ waves, respectively. Among them, the s wave belongs to an identical representation A_1 of D_4 group, the degenerate p_x and p_y waves form a two-dimensional irreducible representation E of D_4 group, and the $d_{x^2-y^2}$ wave belongs to an irreducible representation B_1 of D_4 group.

When $K_x \neq \pm K_y$, $t_{\hat{x}} \neq t_{\hat{y}}$, the symmetry reduces to D_2, a subgroup of D_4. For simplicity, we still label the four bound states with s, $p_{x(y)}$, and $d_{x^2-y^2}$. Differently, here, all the s and d waves belong to identical representations A_1 of D_2 group, while $p_x(p_y)$ wave belongs to an irreducible representation $B_3(B_2)$ of D_2 group. The degeneracy of p_x and p_y waves is lifted.

With $\boldsymbol{\rho}' = (0,0)$, $(\pm 1, \pm 1)$, equation (9) reduces to five linear equations in the two-dimensional case. The free Green function $G_0(\boldsymbol{\rho}, \boldsymbol{\rho}')$ can be expressed with elliptic integrals.[36,39] Although no brief solution of $\langle \boldsymbol{\rho}|G|\boldsymbol{\rho}'\rangle$ could be found, we may factorize the particle–hole bound state equations and analyze the existence conditions for the bound states along the symmetric lines of $K_x = \pm K_y = K$.[39] Considering the asymptotic behaviors of elliptic integrals, we get the thresholds of the interaction V as follows: $V_{\text{cr,s}}(K) = t_{\hat{x}}$ for s wave, $V_{\text{cr,p}}(K) = [2\pi/(2\pi-4)]t_{\hat{x}}$ for $p_{x(y)}$ wave, and $V_{\text{cr,d}}(K) = [2\pi/(8-2\pi)]t_{\hat{x}}$ for $d_{x^2-y^2}$ wave. From these thresholds, the existence region of every bound state is obtained respectively. For s wave, we have

$$2\arccos\sqrt{\frac{V^2-t^2}{8t^2}} \leq |K| \leq \pi, V \in (t, 3t].$$

When $V > 3t$, the s wave bound state may be found in the whole Brillouin zone. The existence region of p-wave bound states is

$$2\arccos\sqrt{\frac{\{[(\pi-2)/\pi]V\}^2 - t^2}{8t^2}} \leq |K| \leq \pi,$$
$$V \in \left(\frac{\pi}{\pi-2}t, \frac{3\pi}{\pi-2}t\right].$$

When $V > [3\pi/(\pi-2)]t$, the existence region extends to the whole Brillouin zone. For d wave, existence region is expressed as

$$2\arccos\sqrt{\frac{\{[(4-\pi)/\pi]V\}^2 - t^2}{8t^2}} \leq |K| \leq \pi,$$
$$V \in \left(\frac{\pi}{4-\pi}t, \frac{3\pi}{4-\pi}t\right].$$

When $V > [3\pi/(4-\pi)]t$, the d-wave existence interval is the whole Brillouin zone.

Now, we present the numerical results in two dimensions. At $\boldsymbol{K} = (0,0)$, four bound states could be found when $V \geq V_{\text{cr,d}}(0) = 10.97t$. The wave functions with s-, p_x-, and $d_{x^2-y^2}$-wave symmetry for $V = 12t$ are shown in Fig. 4. With the decrease of V, the highest d_{x^2-y2}wave, the degenerate $p_{x(y)}$ waves, and the lowest s-wave merge into the continuous spectrum one by one. Finally, all the bound states disappear when $V \leq V_{\text{cr,s}}(0) = 3t$. In Fig. 5, we illustrate the variations of the bound state energies with the changes of V.

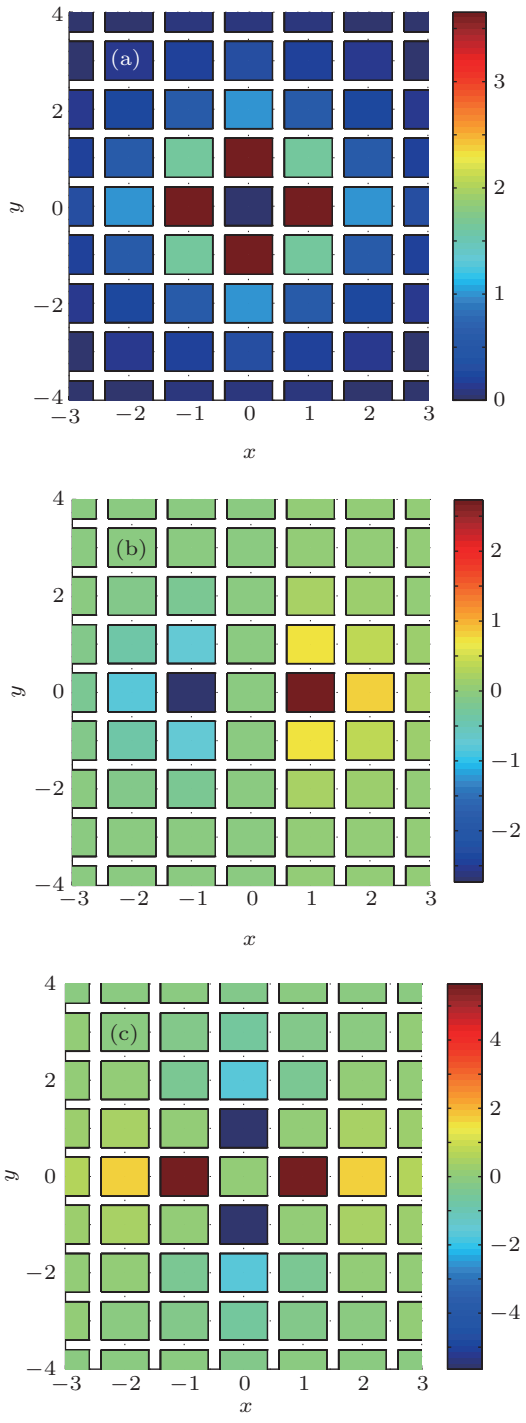


Fig. 4. (color online) The wave functions of bound states in the two-dimensional case at $\boldsymbol{K} = (0,0)$ and $V = 12t$ (non-normalized). (a) s-, (b) p_x-, and (c) $d_{x^2-y^2}$-wave symmetries can be observed respectively.

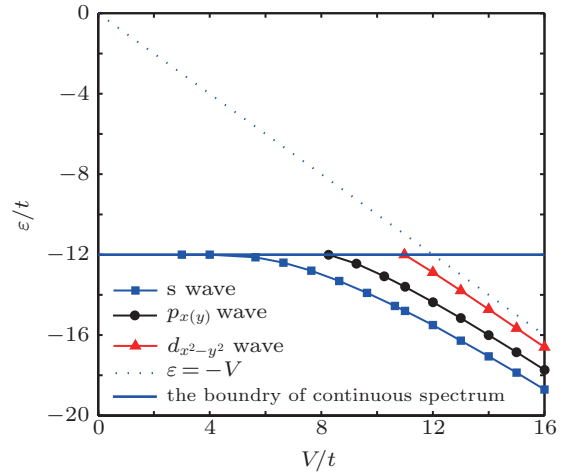


Fig. 5. (color online) Variations of the energies of different bound states in two dimension at $\boldsymbol{K} = (0,0)$. The energies of different bound states increase with the decrease of V and cross the particle–hole continuum [$-12t$ at $\boldsymbol{K} = (0,0)$] at different V.

We then search for bound state solutions along the line of $K_x = K_y = K$. As shown in Fig. 6, there are four bound states for all $K \in [-\pi, \pi]$ at $V = 12t$. At $V = 6t$, s-wave exists in the whole region, while $p_{x(y)}$- and $d_{x^2-y^2}$-wave states appear at $0.52\pi < |K| \leq \pi$ and $0.69\pi < |K| \leq \pi$ respectively. Decreasing V further, we find that the regions of the bound states shrink, and all the bound states disappear when $V < V_{\mathrm{cr,s}}(\pm\pi) = 1t$. Similar results are obtained along the line of $K_x = -K_y = K$.

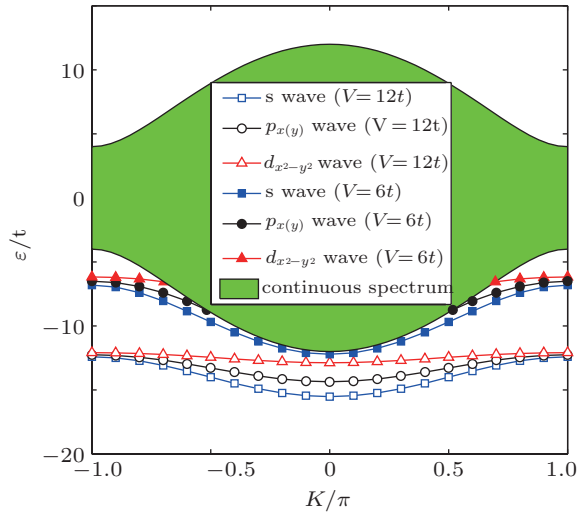


Fig. 6. (color online) Dispersion relations of bound states along the line of $K_x = K_y = K$ for $V = 6t$ and $V = 12t$. As a comparison, the particle–hole continuum is also shown (green shaded region).

Away from the lines of $K_x = \pm K_y$, the degeneracy of p_x and p_y bound states is lifted, as mentioned before. At a given V, different bound states have different existence regions in $\boldsymbol{K}$ space. Consequently, the number of bound states vary in the (K_x, K_y) space. As an example, we show the number distribution of the bound states for $V = 6t$ in Fig. 7.

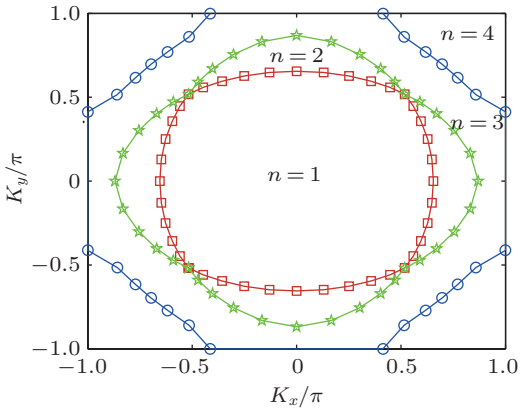


Fig. 7. (color online) The number distribution of bound states in the first Brillouin zone at $V = 6t$. As shown, there are more bound states at the corners than that at the center in the first Brillouin zone.

3.3. Discussion of observations of the bound states

Inelastic light scattering directly measures the dynamical structure factor $S(\boldsymbol{q}, \omega)$, the Fourier transformation of density correlations. Bragg spectroscopy has been proposed to detect quantum phases in an optical lattice and successfully applied to measure the excitation spectra (phonons of BEC), the composition of the excitations, and the Higgs-type amplitude mode in the superfluid condensate, as well as the particle–hole excitation energies in the Mott-insulator state.[40–46] When this technique is utilized in the study of ultra-cold polar molecules in the optical lattice, we may expect extra resonance peaks corresponding to the particle–hole bound states lying outside the particle–hole continuum.

Compared with the traditional solid state counterparts, the deep Mott insulating state with $t/U \ll 1$ and $zV < U$ can be realized by tuning the interaction parameters t, U, and V in ultra-cold dipolar molecules in the optical lattices. In deep optical lattices, the hopping is approximately evaluated as $t = (4/\sqrt{\pi})E_{\mathrm{r}}(V_{\mathrm{opt}}/E_{\mathrm{r}})^{3/4}\exp[-2(V_{\mathrm{opt}}/E_{\mathrm{r}})^{1/2}]$, with $V_{\mathrm{opt}} = 18E_{\mathrm{r}} \sim 20E_{\mathrm{r}}$ the optical lattice depth and E_{r} the lattice recoil energy.[47] Under the condition of $a_{\mathrm{s}}/a_{\perp} \ll 1$, where a_{s} is the s-wave scattering length and $a_{\perp} = \sqrt{\hbar/m\omega_{\perp}}$ with $\omega_{\perp}$ transverse trapping frequency in one dimension or trapping frequency of the z direction in two dimensions, the on-site interaction is estimated as $U_{1\mathrm{D}} = \sqrt{(2/\pi)}\hbar\omega_{\perp}a_{\mathrm{s}}/l_0$ and

$$U_{2\mathrm{D}} = \frac{\sqrt{8\pi}\hbar^2 a_{\mathrm{s}}}{m a_z (2\pi) l_0^2},$$

with $l_0 = (E_{\mathrm{r}}/V_{\mathrm{opt}})^{1/4}(a/\pi)$, and a the lattice constant.[47,48]

Taking Bose molecule ^{23}Na^{7}Li as an example, we may estimate the typical values of t, U, and V for observing the particle–hole bound state. The molecule prepared in the ground state has a permanent electric moment $d = 0.58$ Debye.[49] With a lattice constant $a \sim 0.5$ μm, $a_{\mathrm{s}}/a \sim 0.01$, and the transversal tapping frequency $\omega_{\perp} \sim 2\pi \times 10^4$ Hz, we have $t \sim 1$ nK, $U_{1\mathrm{D}} \sim 25$ nK, and $U_{2\mathrm{D}} \sim 50$ nK. The nearest-

neighbor interaction V can be tuned as $V \sim 10$ nK with an applied electric field.

4. Summary

In summary, we have investigated the bound states of the particle–hole pair resulting from the dipole–dipole interaction between polar molecules in an optical lattice. For a large enough dipole–dipole interaction, two degenerate bound states, which correspond to a particle on the left and the right of a hole, are shown to exist in one dimension. While in the two-dimensional case, four bound states, with s-, $p_{x(y)}$-, and $d_{x^2-y^2}$- symmetries respectively, are found along the lines of $K_x = \pm K_y$. Away from the lines of $K_x = \pm K_y$, the degeneracy between p_x and p_y waves is lifted. With the decrease of the nearest-neighbor interaction V, the energies of the bound states increase and merge into the particle–hole continuum gradually. The wave functions, the dispersion relations, and the existence regions of the bound states are studied in detail. For a given nearest-neighbor V, the number of bound states is different in different regions of $\boldsymbol{K}$ space and a number distribution of bound states is given for the nearest-neighbor $V = 6t$ in two dimensions. The possible experimental observation of the particle–hole bound states is also discussed.

The work will help us to understand the nature of dipole–dipole interaction in cold molecular physics. It is expected that the investigation of the particle–hole bound states in dipolar molecules will simulate further study interest in the cold molecules. On the other hand, our study on the particle–hole bound states in bosonic systems enriches our understanding of elementary excitations in quantum many-body systems and stimulates more research efforts on the bound state phenomena in various systems such as magnets, superconductors, and atomic systems.

References

[1] Carr L D, DeMille D, Krems R V and Ye J 2009 *New J. Phys.* **11** 055049
[2] Dulieu O and Gabbanini C 2009 *Rep. Prog. Phys.* **72** 086401
[3] Jochim S, Bartenstein M, Altmeyer A, Hendl G, Riedl S, Chin C, Denschlag J H and Grimm R 2003 *Science* **302** 2101
[4] Greiner M, Regal C A and Jin D S 2003 *Nature* **426** 537
[5] Volz T, Syassen N, Bauer D M, Hansis E, Dürr S and Rempe G 2006 *Nat. Phys.* **2** 692
[6] Danzl J G, Mark M J, Haller E, Gustavsson M, Hart R, Aldegunde J, Hutson J M and Nägerl H C 2010 *Nat. Phys.* **6** 265
[7] Ni K K, Ospelkaus S, de Miranda M H G, Pe'er A, Neyenhuis B, Zirbel J J, Kotochigova S, Julienne P S, Jin D S and Ye J 2008 *Science* **322** 231
[8] Ospelkaus S, Pe'er A, Ni K K, Zirbel J J, Neyenhuis B, Kotochigova S, Julienne P S, Ye J and Jin D S 2008 *Nat. Phys.* **4** 622
[9] Sage J M, Sainis S, Bergeman T and DeMille D 2005 *Phys. Rev. Lett.* **94** 203001
[10] Wang D, Kim J T, Ashbaugh C, Eyler E E, Gould P L and Stwalley W C 2007 *Phys. Rev. A* **75** 032511
[11] Sawyer B C, Lev B L, Hudson E R, Stuhl B K, Lara M, Bohn J L and Ye J 2007 *Phys. Rev. Lett.* **98** 253002
[12] DeMille D 2002 *Phys. Rev. Lett.* **88** 067901
[13] Büchler H P, Demler E, Lukin M, Micheli A, Prokof'ev N, Pupillo G and Zoller P 2007 *Phys. Rev. Lett.* **98** 060404
[14] Santos L, Shlyapnikov G V, Zoller P and Lewenstein M 2000 *Phys. Rev. Lett.* **85** 1791
[15] Cooper N R, Rezayi E H and Simon S H 2005 *Phys. Rev. Lett.* **95** 200402
[16] Baranov M A, Osterloh K and Lewenstein M 2005 *Phys. Rev. Lett.* **94** 070404
[17] Góral K, Santos L and Lewenstein M 2002 *Phys. Rev. Lett.* **88** 170406
[18] Menotti C, Trefzger C and Lewenstein M 2007 *Phys. Rev. Lett.* **98** 235301
[19] Lin C, Zhao E and Liu W V 2010 *Phys. Rev. B* **81** 045115
[20] Bruder C, Fazio R and Schön G 1993 *Phys. Rev. B* **47** 342
[21] van Otterlo A, Wagenblast K H, Baltin R, Bruder C, Fazio R and Schön G 1995 *Phys. Rev. B* **52** 16176
[22] Niyaz P, Scalettar R T, Fong C Y and Batrouni G G 1994 *Phys. Rev. B* **50** 362
[23] Sengupta P, Pryadko L P, Alet F, Troyer M and Schmid G 2005 *Phys. Rev. Lett.* **94** 207202
[24] Hassan S R, Medici L D and Tremblay A M S 2007 *Phys. Rev. B* **76** 144420
[25] Iskin M and Freericks J K 2009 *Phys. Rev. A* **79** 053634
[26] Pai R V and Pandit R 2005 *Phys. Rev. B* **71** 104508
[27] Chen Y C, Melko R G, Wessel S and Kao Y J 2008 *Phys. Rev. B* **77** 014524
[28] Wang Y M, Liang J Q 2012 *Chin. Phys. B* **21** 060305
[29] Fisher M P A, Weichman P B, Grinstein G and Fisher D S 1989 *Phys. Rev. B* **40** 546
[30] van Oosten D, van der Straten P and Stoof H T C 2001 *Phys. Rev. A* **63** 053601
[31] Kovrizhin D L, Pai G V and Sinha S 2005 *Europhys. Lett.* **72** 162
[32] Gallagher F B and Mazumdar S 1997 *Phys. Rev. B* **56** 15025
[33] Barford W 2002 *Phys. Rev. B* **65** 205118
[34] Al-Hassanieh K A, Reboredo F A, Feiguin A E, González I and Dagotto E 2008 *Phys. Rev. Lett.* **100** 166403
[35] Mattis D C 1981 *The Theory of Magnetism* Vol. I (Berlin–New York: Springer-Verlag)
[36] Economou E N 2006 *Green's Functions in Quantum Physics* 3 edn. (Berlin:Springer-Verlag)
[37] Nygaard N, Piil R and Mølmer K 2008 *Phys. Rev. A* **78** 023617
[38] Barford W 2002 *Phys. Rev. B* **65** 205118
[39] Wortis M 1963 *Phys. Rev.* **132** 85
[40] Ye J W, Zhang J M, Liu W M, Zhang K Y, Li Y and Zhang W P 2011 *Phys. Rev. A* **83** 051604
[41] Stamper-Kurn D M, Chikkatur A P, Görlitz A, Inouye S, Gupta S, Pritchard D E and Ketterle W 1999 *Phys. Rev. Lett.* **83** 2876
[42] van Oosten D, Dickerscheid D B M, Farid B, van der Straten P and Stoof H T C 2005 *Phys. Rev. A* **71** 021601
[43] Rey A M, Blakie P B, Pupillo G, Williams C J and Clark C W 2005 *Phys. Rev. A* **72** 023407
[44] Ernst P T, Götze S, Krauser J S, Pyka K, Lühmann D S, Pfannkuche D and Sengstock K 2010 *Nat. Phys.* **6** 56
[45] Bissbort U, Götze S, Li Y, Heinze J, Krauser J S, Weinberg M, Becker C, Sengstock K and Hofstetter W 2011 *Phys. Rev. Lett.* **106** 205303
[46] Clément D, Fabbri N, Fallani L, Fort C and Inguscio M 2009 *Phys. Rev. Lett.* **102** 155301
[47] Bloch I, Dalibard J and Zwerger W 2008 *Rev. Mod. Phys.* **80** 885
[48] Jaksch D, Bruder C, Cirac J I, Gardiner C W and Zoller P 1998 *Phys. Rev. Lett.* **81** 3108
[49] Mabrouk N and Berriche H 2008 *J. Phys. B: At. Mol. Opt. Phys.* **41** 155101